

# Reflectivity Estimation for SAR Image Compression

Grégoire Mercier, *Member, IEEE*

**Abstract**—Synthetic aperture radar (SAR) images suffer from speckle noise that degrades image quality. Also, speckle removal is needed for lossy image compression as such noise increases image entropy. Nevertheless, most lossy compression schemes act as low-pass filters that might not suit multiplicative noise reduction. In order to build a compression scheme that takes into consideration statistics of SAR images, a well-known reflectivity estimator is integrated into an JPEG 2000-like image compression strategy, so that image compression artifacts may be viewed as an adaptive despeckle filter instead of a simple lowpass filter. It yields a compression algorithm that acts in a similar way to the Lee (or Kuan) filter.

**Index Terms**—Image compression, speckle reduction, synthetic aperture radar (SAR), wavelet transform.

## I. INTRODUCTION

SYNTHETIC aperture radar (SAR) produces data by coherent summation of elementary scattered electromagnetic fields that makes images sensitive to the speckle effect. Common SAR compression strategies act as lowpass filters, since it is considered that noise is located in high frequencies. It has been shown that tools that are efficient for compression (such as the wavelet transform) do not perform reflectivity estimation with the same quality as the linear minimum mean square error (LMMSE) estimator [1]. Simard *et al.* [2] give a complete description of the use of wavelet transforms for multiscale texture analysis. Since wavelets are sensitive to noise, they can be used for speckle noise reduction, as in [3] and [4]. But most wavelet-based speckle reduction methods are based on the use of a homomorphic filter [5] that yields acceptable image enhancement and can suit an image compression scheme built with transform coding, adaptive quantization and entropy encoding [6], since noise is considered as becoming additive.

In this communication, it is proposed to investigate a common filter that performs unbiased reflectivity estimation within an LMMSE estimator (like the Lee or Kuan filter) from a compression point of view. It is expected to achieve strong compression with losses that may be interpreted as the result of speckle reduction. The filter is to be written with the wavelet transform to follow the JPEG 2000 norm [7]. The key to this study is to rewrite the Lee (or Kuan) filter from a filter-bank point of view, so that the wavelet coefficients are locally weighted regarding the scene's homogeneity, before being processed in a compression scheme.

## II. REFLECTIVITY ESTIMATION OVERVIEW

Image formation is achieved for a SAR sensor by many elementary wave scatterers [8]. For a significant number  $N_b$  of backscatters in a homogeneous area of reflectivity  $R$  (fully developed speckle is assumed), it appears that the mean of the intensity of the pixels is proportional to its variance. Thus, speckle noise  $S_I$  is to be considered as multiplicative so that

$$I = E[I]S_I = RS_I \quad (1)$$

with  $I$  denoting pixel intensity and  $E[I]$  its local mean.  $S_I$  is the normalized speckle of mean  $E[S_I] = 1$ .

### A. Lee and Kuan Filters

Assuming reflectivity  $R$  as an stationary and ergodic RV, its estimate can be reached within an LMMSE estimator, written as

$$\hat{R} = E[I] + \kappa(I - E[I]) \quad (2)$$

with

$$\kappa = \frac{1 - \frac{\gamma_S^2}{\gamma_I^2}}{1 + \frac{\gamma_S^2}{\gamma_I^2}} \quad (3a)$$

for the Kuan filter [9] and

$$\kappa = 1 - \frac{\gamma_S^2}{\gamma_I^2} \quad (3b)$$

for the Lee filter [10]. The variation coefficient  $\gamma$  is defined as the standard deviation over mean ratio:  $\gamma_I = \sigma_I/\mu_I$ , and for speckle noise (also called speckle strength):  $\gamma_S = 1/\sqrt{L}$ ,  $L$  being the number of looks.

The basic idea of these filters is to consider  $\hat{R} = E[I]$  on homogeneous areas. In fact,  $\gamma_I \simeq \gamma_S$  and thus  $\kappa \simeq 0$ . Hence, such an estimator acts locally as a mean filter. On the other hand, when the area is to be considered as heterogeneous,  $\gamma_I \gg \gamma_S$  and  $\kappa \simeq 1$ . Here, the best estimate of reflectivity becomes the intensity itself

$$\hat{R} = I$$

for the Lee filter and

$$\hat{R} = \frac{1}{1 + \frac{\gamma_S^2}{\gamma_I^2}}I + \frac{\frac{\gamma_S^2}{\gamma_I^2}}{1 + \frac{\gamma_S^2}{\gamma_I^2}}E[I]$$

for the Kuan filter. That is to say, in the case of heterogeneous areas, the Lee estimator acts locally as the identity filter.

Manuscript received January 7, 2002; revised November 6, 2002.

The author is with the Département Image et Traitement de l'Information, École Nationale Supérieure des Télécommunications de Bretagne, 29285 Brest, France (e-mail: gregoire.mercier@enst-bretagne.fr).

Digital Object Identifier 10.1109/TGRS.2003.810224

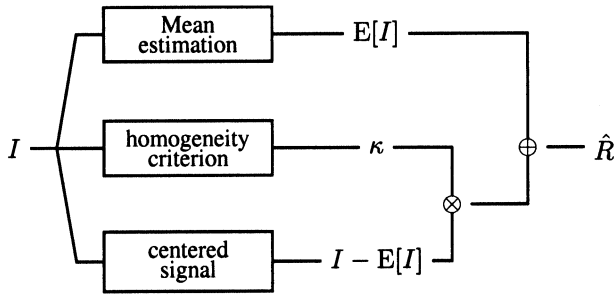


Fig. 1. LMMSE reflectivity estimation flowchart.

### B. Homomorphic Filter

Multiplicative noise may be transformed into additive noise by using of logarithmic transformation

$$\log I = \log R + \log S_I. \quad (4)$$

The estimation of a signal with exponential density after doing a logarithmic transformation is not optimal because it introduces a bias. Nevertheless, when speckle noise and reflectivity may be considered independent, this has the advantage of separating noise from signal. Then, classical additive noise reduction tools may be applied.

An approach for denoising image may be achieved with classical wavelet-based tools and stated as a thresholding of the wavelet coefficients of the noisy image, either hard of soft [11], [12]. The soft-thresholding implies that the modulus of the thresholded coefficient is diminished by the threshold value; it is also widely referred to as *shrinkage* in the literature. However, the noise is assumed to be independent of the noise-free image, gaussian and of zero mean. But it has been shown in [13] that the log-transformed speckle is not gaussian, of nonzero mean that induce bias on reflectivity estimation. In fact, the benefits of this filter appear mostly for visualization.

Instead of shrinking the wavelet coefficients, alternative approach refers to adapted thresholding by using a sigmoid function fully detailed in [6] or [14].

### III. ESTIMATION THROUGH THE WAVELET TRANSFORM

Expectation  $E[I]$  is usually estimated with a square window that acts as a mean filter  $H$ . Then,  $E[I] = H * I$  ( $*$  being the convolution operator). Let  $G$  be defined as the complement of  $H$  so that  $H + G$  is the identity filter. Equation (2) may be rewritten as follows:

$$\hat{R} = E[I] + \kappa(I - E[I]) = H * I + \kappa(G * I) \quad (5)$$

that may be thought of as the result of a filter bank applied on the intensity image (see Fig. 1).

#### A. Multiresolution Analysis (MRA)

The basic idea is to estimate  $E[I]$  in (5) by a mean operator that takes into consideration scene autocorrelation that decreases with pixel distance. Instead of taking the Frost point of view, with the estimation of correlation length, estimation of  $E[I]$  may be achieved through a smooth finite-impulse response lowpass filter that is implemented from an MRA point of view.

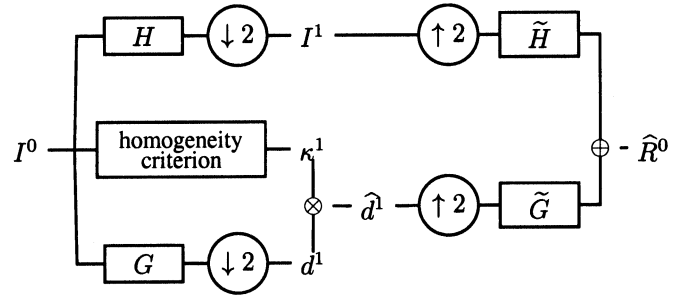


Fig. 2. Wavelet-based reflectivity estimation flowchart.

According to Daubechies' notations [15], the MRA of an image  $I$  at a level  $\ell$  may be expressed as the convolution with a lowpass filter  $H$  and a highpass  $G$ , such that, for  $0 < \ell \leq N$

$$I_j^\ell = \sum_k h_{2j-k} I_k^{\ell-1} \quad d_j^\ell = \sum_k g_{2j-k} I_k^{\ell-1}. \quad (6)$$

The original signal ( $I \stackrel{\text{def}}{=} I^{\ell=0}$ ) may be recovered from the wavelet coefficients by means of the synthesis equation

$$I_j^{\ell-1} = \sum_k \tilde{h}_{2k-j} I_k^\ell + \sum_k \tilde{g}_{2k-j} d_k^\ell \quad (7)$$

where  $\tilde{h}_k$  and  $\tilde{g}_k$  are, respectively, scaling and wavelet coefficients of the dual (biorthogonal) wavelet basis.

#### B. Wavelet-Based Reflectivity Estimation

Estimation of reflectivity  $\hat{R}$  of (5) may then be rewritten with scaling function and wavelet in an MRA in order to estimate wavelet coefficients of reflectivity from the wavelet coefficients of intensity (as shown in Fig. 2). Reflectivity estimation becomes the synthesis of lowpass coefficients  $I^\ell$  and highpass coefficients  $d_k^\ell$  that are locally weighted with  $\kappa^\ell$  (coming from (3) that will be adapted to fit resolution  $\ell$ ). When  $\kappa^\ell$  indicates a homogeneous area,  $\hat{d}_k^\ell = \kappa_k^\ell d_k^\ell$  has to be minimized in order to synthesize smooth texture. On the other hand,  $\hat{d}_k^\ell$  is left equal to  $d_k^\ell$  on heterogenous areas where the best estimate of  $\hat{R}$  is  $I$  itself (taking Lee's point of view)

$$\begin{aligned} \hat{R} &= H * I + \kappa(G * I) \\ \hat{R}_j^0 &= \sum_k \tilde{h}_{2k-j} I_k^1 + \sum_k \tilde{g}_{2k-j} \hat{d}_k^1 \end{aligned} \quad (8)$$

where  $I^1$  (respectively,  $\hat{d}^1$ ) coming from the filtering and decimation of intensity SAR image  $I$  with the filter  $H$  (respectively,  $G$ ). In an MRA,  $I^1$  may itself be reconstructed from  $I^2$  and  $\hat{d}^2$  (locally weighted by  $\kappa^2$ ), and so on. Note that the lowpass part of intensity being untouched, the estimation remains unbiased. For this wavelet-based estimation, the mother wavelet 9/7, that is included in the JPEG 2000 compression norm [7], was used.

The weighting coefficient  $\kappa$  may now be evaluated from an MRA point of view instead of the original (3). Two strategies may be developed.

- 1) *Estimation from Finer Scale (EFS)*. On the one hand, the evaluation may be achieved in the wavelet domain. At each level  $\ell$  ( $0 \leq \ell < N$ ) the variation coefficient of intensity  $I^\ell$  may be obtained from  $\gamma_{I^\ell} = \sigma_{I^\ell} / \mu_{I^\ell}$ . When

TABLE I  
RESULTS OF SPECKLE REDUCTION ON SIMULATED HOMOGENEOUS IMAGES  
WITH CONSTANT OR  $K$ -DISTRIBUTED REFLECTIVITY

		Constant Reflectivity				$K$ -distributed	
		mean	$L_{eq}$	mean	$L_{eq}$	mean	$L_{eq}$
original	(a)	95.42	2.97	478.9	2.99	83.5	3.12
Lee	(b)	95.4	14.3	478.9	14.6	83.5	16.0
soft-thres	(c)	91.1	148	457.6	156	80.3	193
sigmoid-thres	(d)	91.1	125	457.6	138	80.3	170
wvlt-EFS	(e)	95.42	122	478.9	129	83.5	167
wvlt-EOI	(f)	95.42	120	478.9	127	83.5	166

speckle noise is filtered with a lowpass filter, one can prove that  $L$  is increased by a factor of  $\sqrt{2}$  at each scale, since  $H(z=0) = \sqrt{2}$  in the wavelet context. Thus,  $\gamma_{S^\ell} = 1/\sqrt{2^\ell L}$  and the weighting coefficient becomes  $\kappa^{\ell+1} = 1 - \gamma_{S^\ell}^2/\gamma_{I^\ell}^2$ .

2) *Estimation from the Original Image (EOI)*. On the other hand, the evaluation of  $\kappa^\ell$  may be achieved by manipulating initial intensity data  $I$  and using windows of a size linked with the dilatation of the mother wavelet.  $\gamma_{S^\ell}$  remains equal to  $1/\sqrt{L}$ , since speckle noise is considered as stationary, whereas  $\gamma_{I^\ell}$  is evaluated with  $\gamma_{I^\ell}/\mu_{I^\ell}$  by using a square window increasing in size as  $\ell$  grows from 0 to  $N - 1$ . This latter solution gives better results as the smoothing effect is more efficient on homogeneous areas. Nevertheless, edges may be blurred and an edge detector  $r$  with  $r \in [0, 1]$ , such as the Touzi means ratio [16] may be used to weight  $\kappa^\ell$  with  $(\kappa_k^\ell)^{(1-r)}$ ;  $r = 0$  means a homogeneous area, while  $r = 1$  indicates an edge detected. So estimation of the reflectivity wavelet coefficients becomes

$$\hat{d}_k^\ell = (\kappa_k^\ell)^{(1-r)} d_k^\ell.$$

#### IV. RESULTS ON ESTIMATION

##### A. Simulated Images

Reflectivity estimations were first applied to simulated radar images. Later, they will be applied to images, with forestry applications, from the Precision Image mode (PRI) of the European Remote Sensing (ERS) satellite. Since PRI mode yields three-look images, simulations are achieved in such a way as to yield three-look intensity images.

The simulation procedure was inspired by radar image formation phenomena. Each pixel is simulated with a given amplitude  $A$  and hundreds of phases  $\phi_n$  coming from independent uniform generations in  $[0, 2\pi]$  to characterize elementary wave scatterers. Taking the square of the module of each pixel yields a one-look intensity image. A three-look intensity image is obtained by averaging tree adjacent pixels. A three-region image was generated this way with two constant value reflectivity areas (100 and 500) and an area where amplitude  $A$  of each pixel came from a gamma distribution. This induces a  $K$ -distributed intensity image that suits natural forest statistics. All these three regions are approximately three-look.

Table I show the results of reflectivity estimation on the three homogeneous areas. The Lee filter was implemented with a

window of size  $7 \times 7$  which corresponds to the length of the mother wavelet used in the wavelet-based methods. It is also the size of the window used in the EFS methods for estimating the speckle strength. When the window size increases, the Lee filter yields similar results to the one obtained when using a window of  $7 \times 7$ .

Soft- and Sigmoid-thresholding approaches show, as expected in [13], a systematic bias in the reflectivity estimation. Instead of assuming a noise standart deviation of  $\sigma = \sqrt{1/3}$  as it is the case for the Lee filter, the log-transform has been taken into consideration, and  $\sigma$  has been fixed to  $\Psi(1, L)$  where  $\Psi(\cdot)$  is the digamma function. Those two algorithms are minimizing the magnitude of the wavelet coefficients relatively to a global threshold, then coefficients are vanished through the shrinkage (or the sigmoid weighted) on each homogeneous regions. It results a very efficient filtering, since  $L_{eq}$  grows up to 100 on Table I lines (c) and (d). The wavelet-based implementations of the Lee filter are unbiased (lines (e) and (f) of Table I), with a filtering power as high as the sigmoid-thresholding ( $L_{eq}$  up to 100).

##### B. ERS-PRI Images

Reflectivity estimations were applied to ERS-PRI images acquired over rice fields near Mana (French Guiana). These images are part of a database that is dedicated to the study of the impacts of anthropic activities on the natural forest (deforestation and development) over long periods. Fig. 3(a) shows a  $256 \times 640$  imagette where the items of interest are a river, roads, rice fields (a few of them with low radiometry are flooded), and textured forest. Another region of interest (of 10 000 pixels) was selected to evaluate the equivalent number of looks ( $L_{eq}$ ) in a homogeneous area. Fig. 3(b) shows the results of the Lee filter. It will be used as a reference for the wavelet-based filters, since the latter follow the same LMMSE estimation formalism.

The log-transform-based approach, shown on (c) and (d), have been using a speckle standart deviation of  $\sigma = \Psi(1, L) \approx 0.895$  instead of the usual  $\sigma = \sqrt{1/L}$ . In a similar way as for the simulated images, wavelet-based soft- and sigmoid-thresholding [respectively, (c) and (d)] gives characteristic visual artifacts, and Table II underlines the bias in the mean estimation of the homogeneous area.

The wavelet-based LMMSE estimators respectively implemented with the EFS (e) and EOI (f) methods allow a more accurate restitution of fine details (Hedges between rice fields, banks of the river). Even if the local detection of homogeneity is given by the  $\kappa$  coefficients, the filtering effect is much stronger than the original Lee filter.  $L_{eq}$  was founded equal to 5.95 with the Lee filter while founded as high as 27.6 and 85.4 with those filters.

#### V. COMPRESSION

Instead of estimating reflectivity from a SAR image through an MRA with scalar or vector wavelets, that are filtered according to (8), it is possible to split the process and compress the filtered wavelet coefficients  $\hat{d}_k^\ell$ . It results a compression scheme that acts as a speckle removal filter.

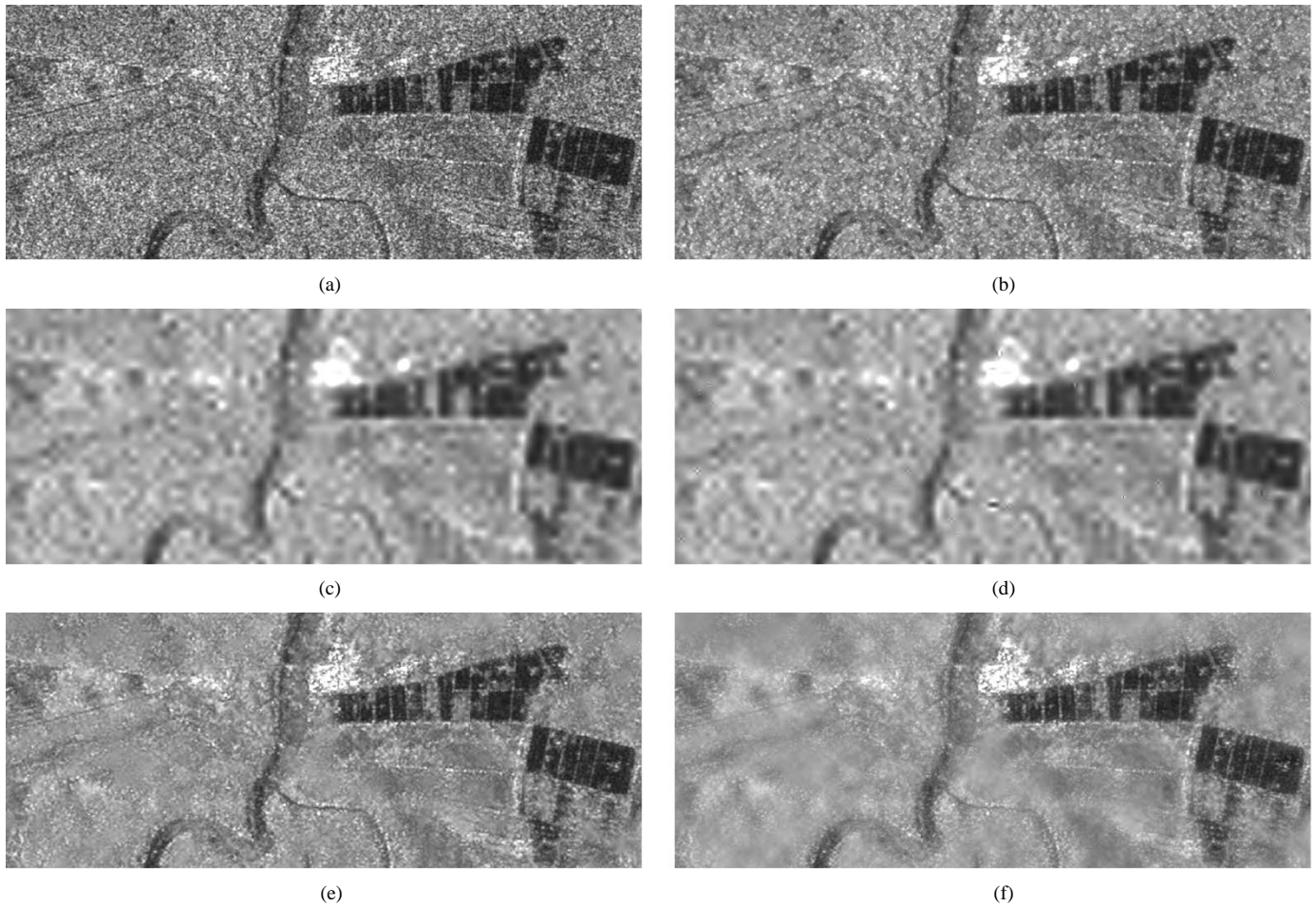


Fig. 3. Filtering results on ERS-1 image. See also Table II.

TABLE II  
RESULTS OF SPECKLE REDUCTION ON ERS-PRI SAR IMAGE

	Fig. 3	mean	$L_{eq}$
original	(a)	387.4	2.98
Lee	(b)	387.31	9.11
soft-thres	(c)	370.8	33.36
sigmoid-thres	(d)	370.8	33.2
wvlt-EFS	(e)	387.2	27.6
wvlt-EOI	(f)	387.2	85.4

### A. Quantization

Weighted wavelet coefficients are simply scalar quantized using the embedded quantizer fully described in [17]. So the compression scheme remains compatible with the JPEG 2000 recommendations. This quantization technique is based on layered quantizers. Symbols coming from quantizer  $Q_1$  are encoded into the layer  $\mathcal{L}_1$ , while the information necessary to recover symbols from quantizer  $Q_n$  ( $1 < n \leq Q$ ,  $Q$  being the total number of quantizers), given that all quantizers  $Q_1, \dots, Q_{n-1}$  are already known, are encoded into the layer  $\mathcal{L}_n$ .

Multilayered quantization is associated with adaptive entropy coding. The encoder performs arithmetic encoding and is designed for use with the quantizer above, since significant and insignificant symbols (according to a quantization level  $\mathcal{L}_n$ ) are treated separately.

TABLE III  
NUMERICAL RESULTS ON COMPRESSION AND JOINT FILTERING AND COMPRESSION OF THE ERS-PRI IMAGE. SEE FIG. 4 FOR VISUAL EVALUATION AT A COMPRESSION RATE OF  $\eta = 40 : 1$ 

		Compression rate $\eta$						
		see also Fig. 4	0	10	20	40*	60	100
ori	(a)	$L_{eq}$	2.98	3.1	3.6	4.8	5.8	6.8
		$SNR_{ori}$	n/a	11.65	7.25	5.05	3.99	3.14
		$L_{eq}$	9.1	9.6	10.9	13.4	15.9	20.9
Lee	(b)	$SNR_{ori}$	8.04	6.85	5.47	4.18	3.44	2.87
		$SNR_{flt}$	n/a	14.19	10.18	7.81	6.67	5.70
		$L_{eq}$	27.6	28.1	30.3	36.1	42.7	54.1
wvlt-EFS	(c)	$SNR_{ori}$	5.26	5.01	4.43	3.73	3.20	2.65
		$SNR_{flt}$	n/a	21.37	14.76	10.88	8.99	7.45
		$L_{eq}$	85.3	88.3	90.8	92.3	95.0	96.3
wvlt-EOI	(d)	$SNR_{ori}$	3.17	3.03	2.80	2.46	2.27	1.97
		$SNR_{flt}$	n/a	22.59	17.24	13.77	12.41	10.81

\* See Fig. 4 for visual evaluation at a compression rate of  $\eta = 40 : 1$ .

A bit allocation technique controls quantizer parameters. It is based on integer programming algorithms described in [18]. The goal of this bit allocation step is to distribute a quota of bits to a set of quantizers that do not have *a priori* the same performance (in the distortion-rate sense).

### B. Quantization Effects on Estimation

From a denoising point of view, the quantization procedure may seem to be a multilevel thresholding. Then, multilayered

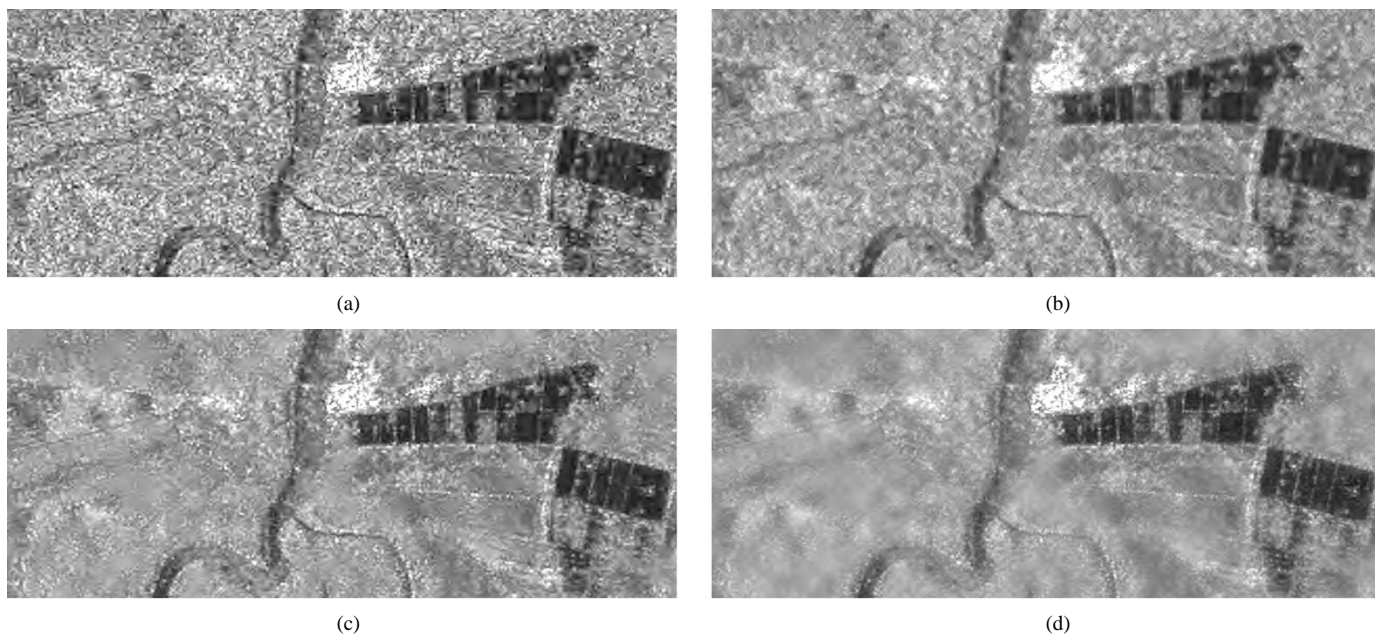


Fig. 4. Results on compression mixed with reflectivity estimation approach at a compression rate of  $\eta = 40 : 1$ . See also Table III.

quantization may be expressed as an encapsulated hard-thresholding that uses increasing thresholds  $T_{\mathcal{L}_1}, T_{\mathcal{L}_2}, \dots, T_{\mathcal{L}_Q}$ . Such a quantization acts as a lowpass-based denoising procedure that suits additive zero-mean noise. The equivalent number of looks is affected by the quantization artifacts. The higher the compression ratio, the more the reflectivity estimation is biased.

At decoding, only the  $T_{\mathcal{L}_i}$ ,  $0 < i \leq Q$  (that is to say, the quantization tables) are needed to retrieve wavelet coefficients properly. Then, image reconstruction is achieved in a standard way with dequantization and an inverse wavelet transform. The reconstruction step does not require knowledge of SAR image statistics and follows JPEG 2000 recommendations [7].

## VI. RESULTS ON COMPRESSION

The compression scheme was applied on the ERS-PRI image with various compression ratios (from  $\eta = 10 : 1$  to  $100 : 1$ , i.e., rates of 1.6–0.16 bits per pixel). The goal is to show the benefit of mixing the compression scheme and the estimation process in order to consider the compression artifacts as coming mostly from the speckle removal.

As shown in Table III, compression of Section V was applied on the original image (a) and the Lee-filtered one (b). Mixed compression and estimation were applied on the original image by using the wavelet-based approaches (line (c) for the EFS method, (d) for the EOI). In the mixed approach, the wavelet coefficients are first locally weighted by the  $\kappa$  coefficients before being quantized as describe in Section V. Two quality evaluations are shown: a distance measurement of the compressed image to the original ERS image (denoted “ $\text{SNR}_{\text{ori}}$ ” in Table III) and a distance measurement of the compressed image to the filtered image without compression (denoted “ $\text{SNR}_{\text{flt}}$ ”). Those two measurements allow to balance the impacts of the compression with the ones of the speckle removal.

It appears that the reconstructed images after compression are of better quality (according to the SNR) when compared to

the filtered image (with the same algorithm and same parameters) instead of the original. This indicates that the effects of the compression remains limited regarding to the filtering power. Also, the benefit increases when using MRA-based estimator instead of the Lee filter. In fact, the  $\kappa$  weightening strategy of the wavelet coefficients acts as a preprocessing step that reduces the dispersion of the coefficients and then the compression artifacts.

Fig. 4 shows the imagette of ERS-PRI image compressed at  $\eta = 40 : 1$  where the artifacts of the mixed filtered/compressed image are less important than the ones obtained with the compression of the original image or the image filtered by the Lee filter.

## VII. CONCLUSION

The goal of this study was to include a speckle removal filter into a compression strategy in order to build a compression algorithm that is adapted to the compression of SAR images and for which artifacts may be viewed as coming mostly from a despeckling effect.

Then, an LMMSE reflectivity estimator has been adapted to fit MRA approach, since MRA is known to be the best strategy for compressing images and is the base of the algorithms included in the JPEG 2000 norm. Instead of others wavelet-based speckle removal strategy, the proposed scheme is unbiased and follows the same hypothesis as the ones of the Lee filter.

When adapted to the wavelet transform, the homogeneity estimator  $\kappa$  that comes from the LMMSE estimator may be implemented with two strategies. A recursive estimation considering across scale speckle behavior (EFS method) or a more classical estimator of the speckle strength from the original image (EOI). The filtering efficiency of the EFS method is less significant than EOIs but keeps edges with a better accuracy, while EOI tends to blur edges and suffers from the Gibbs oscillations.

The compression strategy, that remains obvious to be JPEG 2000-compatible, does not induce significant distortion to the filtered image. Then, when a despeckle procedure is to be applied in a thematic, a joint compression may be used for storage or transmission facilities without becoming appalling for end-users.

#### ACKNOWLEDGMENT

The author would like to thank J.-P. Rudant for his generous offer of various data, which made this analysis possible, especially ERS images belonging to the European Space Agency and which were acquired thanks to project number A03\_160, associated with the University of Marne La Vallée, France.

#### REFERENCES

- [1] E. Herve, R. Fjørtoft, P. Marthon, and A. Lopès, "Comparison of wavelet-based and statistical speckle filters," *SAR Image Analysis, Modeling and Techniques III*, ser. Proc. SPIE, vol. 2497, 1998.
- [2] M. Simard, G. DeGrandi, K. Thomson, and G. Bénié, "Analysis of speckle noise contribution on wavelet decomposition of SAR images," *IEEE Trans. Geosci. Remote Sensing*, vol. 36, pp. 1953–1962, Nov. 1998.
- [3] S. Foucher, G. Bénié, and J.-M. Boucher, "Unsupervised multiscale speckle filtering," in *Proc. ICIP*, vol. 1, 1996, pp. 391–394.
- [4] Y. Dong, A. Milne, and B. Forster, "Toward edge sharpening: A SAR speckle filtering algorithm," *IEEE Trans. Geosci. Remote Sensing*, vol. 39, pp. 851–863, Apr. 2001.
- [5] J. E. Odegard, H. Guo, M. Lang, C. S. Burrus, R. O. Wells, L. M. Novak, and M. Hielt, "Wavelet-based SAR speckle reduction and image compression," *Proc. SPIE*, vol. 2487, pp. 259–271, 1995.
- [6] J. Sveinsson and J. Benediktsson, "Speckle reduction and enhancement of SAR images in the wavelet domain," in *Proc. IGARSS*, vol. 1, 1996, pp. 63–66.
- [7] ISO/IEC, "Coding of still picture, JPEG2000 Part I final committee draft, Version 1.0," ISO/IEC JTC 1/SC 29/WG 1 (ITU-T SG8), 2000.
- [8] F. Henderson and A. Lewis, Eds., *Principles and Applications of Imaging Radar*: Amer. Soc. Photogrammetry and Remote Sensing, 1998.
- [9] D. Kuan, A. Sawchuk, T. Strand, and P. Chavel, "Adaptive noise smoothing filter for images with signal-dependent noise," *IEEE Trans. Pattern Anal. Machine Intell.*, vol. PAMI-7, pp. 165–177, Mar. 1985.
- [10] J.-S. Lee, "Speckle analysis and smoothing of synthetic aperture radar images," *Comput. Graph. Image Process.*, vol. 17, pp. 24–32, 1981.
- [11] D. Donoho, "De-noising by soft-thresholding," *IEEE Trans. Inform. Theory*, vol. 41, pp. 613–627, May 1995.
- [12] H. Guo, J. Odegard, M. Lang, R. Gopinath, I. Selesnick, and C. Burrus, "Wavelet based speckle reduction with application to SAR based ATD/R," in *Proc. ICIP*, 1994.
- [13] H. Xie, L. Pierce, and F. Ulaby, "Statistical properties of logarithmically transformed speckle," *IEEE Trans. Geosci. Remote Sensing*, vol. 40, pp. 721–727, Mar. 2002.
- [14] J. Sveinsson and J. Benediktsson, "Review of applications of wavelets in speckle reduction and enhancement of SAR images," *Image and Signal Processing for Remote Sensing VII*, ser. Proc. SPIE, vol. 4541, 2001.
- [15] I. Daubechies, *Ten Lectures on Wavelets*. Philadelphia, PA: SIAM, 1992.
- [16] R. Touzi, A. Lopès, and P. Bousquet, "A statistical and geometrical edge detector for SAR images," *IEEE Trans. Geosci. Remote Sensing*, vol. 26, pp. 764–773, Nov. 1988.
- [17] D. Taubman and A. Zakhor, "Multirate 3-D subband coding of video," *IEEE Trans. Image Processing*, vol. 3, pp. 572–588, Sept. 1994.
- [18] Y. Shoham and A. Gersho, "Efficient bit allocation for an arbitrary set of quantizers," *IEEE Trans. Acoust., Speech, Signal Processing*, vol. 69, pp. 1445–1453, Sept. 1988.